ESO-TP-73G

10

FERMILAB

DEC 23 1997

Longitudinal Dispersion Compensation for the Very Large Telescope Interferometer

Samuel Lévêque , Bertrand Koehler, Oskar von der Lühe

European Southern Observatory
Karl Schwarzschild Str.2
D-85748 Garching bei München

ESO-TP-73G

Abstract

The Very Large Telescope Interferometer [1,13] will be operated in air which will introduce small optical path fluctuations due to internal turbulence [4,6] and dispersion effects. Both may contribute to fringe contrast decrease. Longitudinal dispersion effects can be corrected by inserting an appropriate glass of variable thickness in one arm of the interferometer [3,5,11,12]. This paper presents a new method applied to VLTI in order to select the optimum glass, according to both the observing wavelength and the spectral bandpath, and to calculate its thickness. Results are presented in terms of improvement on the fringe contrast.

1. Introduction

In order to obtain fringes from a distant astronomical source with an interferometer which consists of several independent telescopes, the optical paths as seen from the object while propagating through individual telescopes towards a common beam combiner must be equalised. Thus, depending on the sky coordinates of the object, its diurnal motion, and the baseline of the interferometer, an internal delay is continuously adjusted to balance the two optical paths. VLTI will use a Cat's eye configuration with a total stoke of 60m.

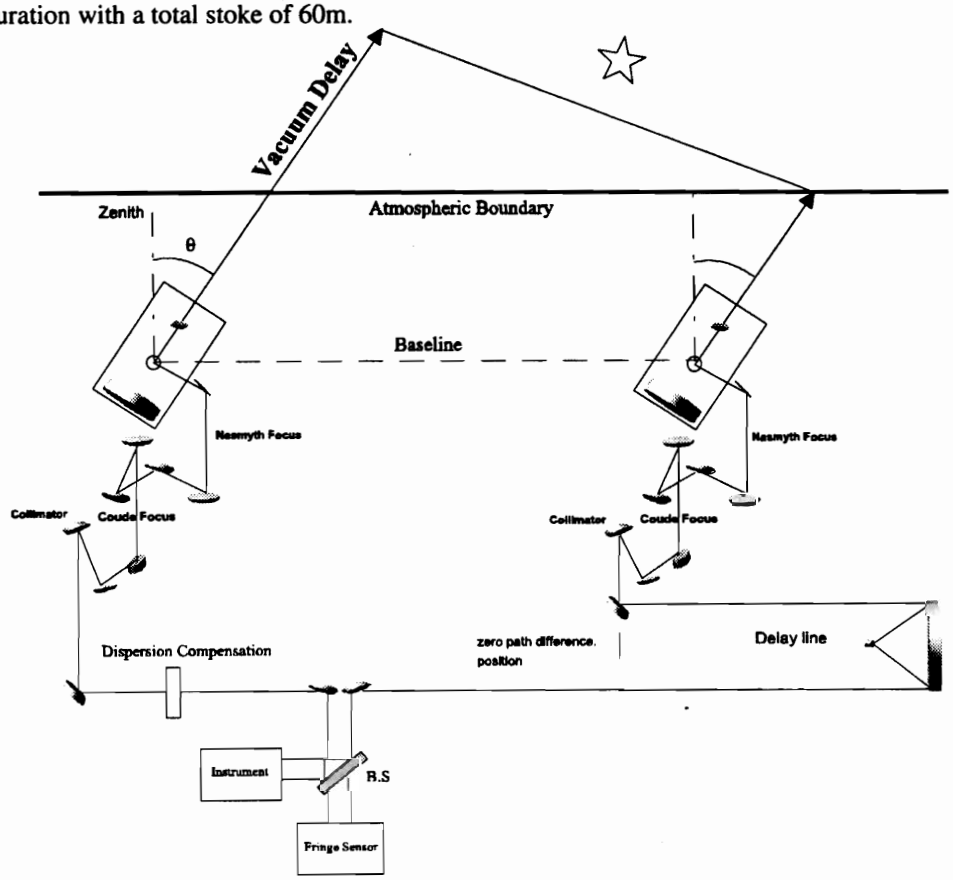

Fig. 1: Sketch of a 2 telescopes interferometer.

Fermilab Library
0 1160 0094449 7

Figure 1 shows that, when telescopes are pointing towards the same source, the optical path difference occurs before reaching the earth's atmosphere, i.e. in vacuum. Therefore the paths travelled by the star light through the atmosphere down to the telescopes are the same. For delay lines operating in air, a differential air path equal to twice the position of the delay line carriage occurs in addition to any imbalance in the path length.

In the case of VLTI, a dedicated sub-system, the Fringe Sensor [2], will allow to position the delay lines in closed loop to maximise the fringe contrast in the H band by observing the source under study or a nearby reference star. The fringe sensor will be operated at λ_{Fs} =1.6μm and will be able to sense the group delay. Therefore, the group optical path difference taken at the fringe sensor operating wavelength, $OPD_g(\lambda_{Fs})$, will be cancelled.

Let us assume that the fringe sensor and the instrument are equidistant from a dispersion free beam splitter. The phase optical path difference, as seen by an instrument observing at λ, is related to the phase optical path difference at λ_{Fs} by

$$OPD_\lambda = \frac{n_\lambda}{n_{\lambda_{Fs}}} \cdot OPD_{\lambda_{Fs}} + R_\lambda \qquad (1)$$

where R_λ is the residual optical path difference between λ_{Fs} and λ

$$R_\lambda = \left[1 - \frac{n_\lambda}{n_{\lambda_{Fs}}}\right] \cdot D \qquad (2)$$

D represents the vacuum delay which depends on the star coordinates and the baseline. *n* is the refractive index of air taken at wavelength λ, pressure P, and temperature T. According to mean atmospheric conditions observed on the VLT site, we took P=743 mb and T=289 °K and considered a dry CO_2 free air. The air index of refraction has been computed using the formula given by J.C. Owens [8]. Figure 2 shows R_λ for λ_{Fs}=1.6μm and for delays up to 120m.

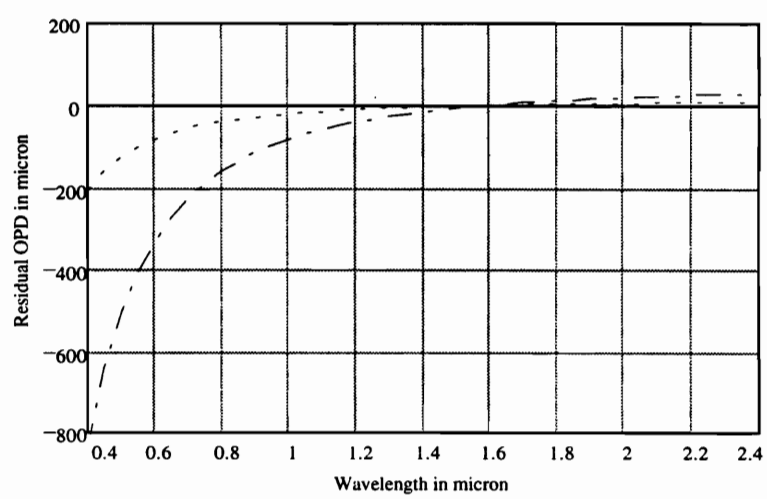

Fig. 2: Residual OPD for 2 vacuum delays: 30m (dotted line) and 120m (dashed line).

Even if $OPD_g(\lambda_{Fs})$ is cancelled by a proper positioning of the delay lines, the stellar fringes appear shifted and the contrast drops for an instrument observing at a wavelength λ different from λ_{Fs}. This phenomenon increases with the delay. The next section will quantify this contrast loss and also include the effect the observing spectral bandwidth.

2. Dispersion effect on fringe contrast

We will now express the information of the residual optical path difference, R_λ , in terms of fringe contrast loss for an observation in the spectral band centred on $\lambda_{obs} = (\lambda_1+\lambda_2)/2$ with a bandwidth $\Delta\lambda=\lambda_2-\lambda_1$. The intensity measured in the output of the interferometer at a given wavelength λ can be written as:

$$I_\lambda = 2 \cdot I_0 \cdot \left[1 + V_0 \cdot \cos\left(\frac{2\pi}{\lambda} OPD_\lambda\right)\right] \qquad (3)$$

However the total detected intensity, within a given bandpass $\Delta\lambda$, depends on the source spectral distribution $S(\lambda)$ and is equal to $I_T = \int_\infty S(\lambda) \cdot I_\lambda \partial\lambda$.

To simplify our discussion, we took a box like spectral distribution ($S(\lambda)=1$ for λ within the bandwidth, $S(\lambda)=0$ elsewhere). We have assumed that both arms receive the same intensity I_o. The star visibility is noted V_o . In order to emphasis the effect of dispersion, we assume that I_o and V_o do not depend on the wavelength within the observing bandwidth.

According to equations (1) and (2) the total detected intensity within the observing bandwidth $\Delta\lambda$ becomes

$$I_T = 2 \cdot I_0 \cdot \left[1 + \frac{V_0}{\Delta\lambda} \cdot \int_{\lambda 1}^{\lambda 2} \cos\frac{2\pi}{\lambda} \cdot \left(\frac{n_\lambda}{n_{\lambda_{Fs}}} . OPD_{\lambda_{Fs}} + R_\lambda\right) \cdot d\lambda\right] \qquad (4)$$

We note that $OPD_{\lambda_{Fs}}$ depends on the fringe sensor operating wavelength and not on λ. The air index of refraction at λ is contained in R_λ and the integral reflects the variation of R_λ across the observing bandwidth.

2.1. Narrow Bandwidth

The contrast loss can be derived in a more straightforward way in the case of a narrow observing window where λ is close to λ_{obs} . The factor $OPD(\lambda_{Fs})$. $2\pi/\lambda_{obs}$ can be pulled out of the integral (4) and considering that $\frac{n_{\lambda_{obs}}}{n_{\lambda_{Fs}}} \approx 1$, I_T can be expressed as:

$$I_T = 2 \cdot I_0 \cdot \left[1 + \frac{V_0}{\Delta\lambda} \cdot \cos\left(\frac{2\pi}{\lambda_{obs}} . OPD_{\lambda_{Fs}}\right)\alpha - \frac{V_0}{\Delta\lambda} \cdot \sin\left(\frac{2\pi}{\lambda_{obs}} . OPD_{\lambda_{Fs}}\right) \cdot \beta\right] \qquad (5)$$

where

$$\alpha = \int_{\lambda 1}^{\lambda 2} \cos\left(\frac{2\pi}{\lambda} \cdot R_\lambda\right) \cdot d\lambda \qquad \text{and} \qquad \beta = \int_{\lambda 1}^{\lambda 2} \sin\left(\frac{2\pi}{\lambda} \cdot R_\lambda\right) \cdot d\lambda$$

Finally, equation (5) can be re-written as

$$I_T = 2 \cdot I_0 \cdot \left[1 + \frac{V_0}{\Delta\lambda} \cdot \sqrt{\alpha^2 + \beta^2} \cdot \cos\left(\frac{2\pi}{\lambda_{obs}} \cdot OPD_{\lambda_{Fs}} + \phi\right)\right] \qquad \text{with } \phi = Arctg\left(\frac{\beta}{\alpha}\right) \qquad (6)$$

By comparing equations (3) and (6), the observed contrast due to dispersion effects for a narrow bandwidth is $V_o . V_N$ where

$$V_N = \frac{\sqrt{\alpha^2 + \beta^2}}{\Delta\lambda} \qquad (7)$$

The optical path difference variation across the bandwidth is included in α and β.

2.2. Large Bandwidth

Equation (7) cannot be applied for a large observing window where the approximation $\lambda \approx \lambda_{obs}$ is no longer valid. The expression of the contrast cannot be easily determined by writing the total detected intensity in the form of equation (6). In order to recover the dispersion effects on the contrast, we compared the Taylor expansion of I_T for small values of $OPD_{\lambda_{Fs}}$ in two cases: with and without dispersion.

First, without any dispersion, $R_\lambda=0$, and the intensity given by (4) is written in term of a constant phase μ and the optical path difference at λ_{Fs}, which does not depend on the observing spectral window.

$$I_T = 2 \cdot I_0 \cdot \left[1 + \frac{V_0}{\Delta\lambda} \cdot \int_{\lambda 1}^{\lambda 2} \cos\left(\frac{2\pi}{\lambda} \cdot \left(OPD_{\lambda_{Fs}} + \mu \right) \right) \cdot d\lambda \right] \tag{8}$$

For small values of $OPD(\lambda_{Fs})$, equation (8) is expanded in series

$$I_T = 2 \cdot I_0 \cdot \left[1 + V_0 \cdot \cos\mu \;\; + \; V_o \cdot \left(-\frac{2\pi}{\Delta\lambda} \cdot \ln\frac{\lambda_2}{\lambda_1} \right) \cdot \sin\mu \cdot OPD_{\lambda_{Fs}} + \Theta\left(OPD_{\lambda_{Fs}}{}^2 \right) \right] \tag{9}$$

Secondly, in the presence of dispersion, we expand equation (4) in series for small values of $OPD(\lambda_{Fs})$. With the help of the relation:

$$\cos\frac{2\pi}{\lambda} \cdot \left(OPD_{\lambda_{Fs}} + R_\lambda \right) = \left(1 - \frac{2\pi^2 OPD_{\lambda_{Fs}}{}^2}{\lambda^2} \right) \cdot \cos\left(\frac{2\pi}{\lambda} \cdot R_\lambda \right) - \frac{2\pi}{\lambda} \cdot OPD_{\lambda_{Fs}} \sin\left(\frac{2\pi}{\lambda} \cdot R_\lambda \right)$$

Equation (4) becomes

$$I_T = 2 \cdot I_0 \cdot \left[1 + V_0 \cdot \alpha + V_0 \cdot \delta \cdot OPD_{\lambda_{Fs}} + \Theta\left(OPD_{\lambda_{Fs}}{}^2 \right) \right] \tag{10}$$

where $\alpha = \int_{\lambda 1}^{\lambda 2} \cos\left(\frac{2\pi}{\lambda} \cdot R_\lambda \right) \cdot d\lambda$ and $\delta = \int_{\lambda 1}^{\lambda 2} -\frac{2\pi}{\lambda} \cdot \sin\left(\frac{2\pi}{\lambda} \cdot R_\lambda \right) \cdot d\lambda$

Finally, by comparing equations (9) and (10), the effect of dispersion on the contrast, for large observing window can be written

$$V_L = \frac{1}{\Delta\lambda} \cdot \left[\alpha^2 + \delta^2 \cdot \left(\frac{\Delta\lambda}{-2\pi \; \ln\left(\frac{\lambda_2}{\lambda_1} \right)} \right)^2 \right]^{\frac{1}{2}} \tag{11}$$

For $\lambda_2 \approx \lambda_1$, equation (11) leads to (7), as expected. The coefficients α and δ are computed numerically and include the optical path difference between λ_{Fs} and λ_{obs} as well as its variation across the bandwidth. Figure 3 shows the variations of V_L as a function of the vacuum delay D.

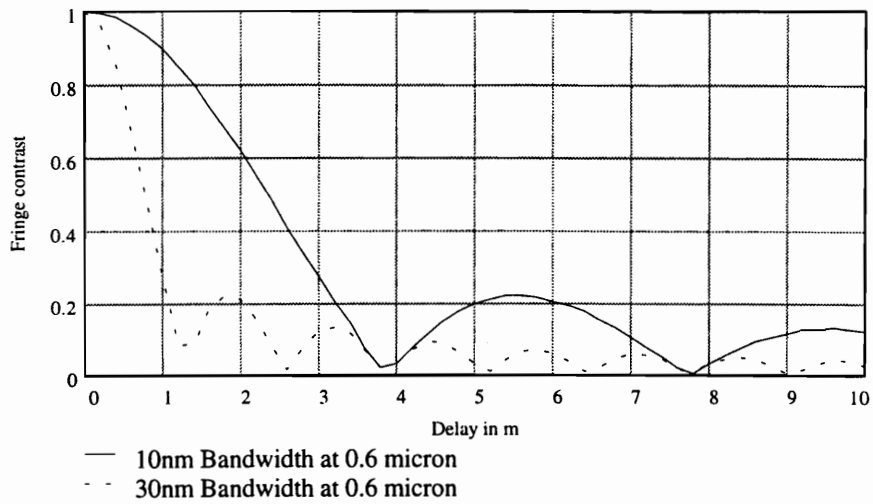

Fig. 3: Dispersion effects on the fringe contrast for 2 bandwidth, without any compensation. The "ringing" is a consequence of the boxcar spectral distribution assumed here.

3. Minimal slope compensation method

If we introduce in the shortest arm of the interferometer, a glass window of thickness T whose index of refraction is noted N_λ, the residual optical path difference presented in equation (2) becomes:

$$R_{G,\lambda}=\left[1-\frac{n_\lambda}{n_{\lambda_{Fs}}}\right]\cdot D+T\cdot\left[N_\lambda-\frac{n_\lambda}{n_{\lambda_{Fs}}}\cdot N_{\lambda_{Fs}}\right] \tag{12}$$

where the second term depends on the characteristics of the glass correction used to balance dispersion effects.

We investigated several methods to find an appropriate glass whose thickness is tuned in order to minimise longitudinal dispersion i.e. to obtain the best fringe visibility, and found the one described here to work best for us. This final result strongly depends on observing conditions through the parameters λ_{obs} and $\Delta\lambda$, as shown in equations 7 and 11, and are included in the selection procedure.

3.1. Minimisation of slope

We impose two conditions on the residual optical path difference after glass correction: the first and second derivatives of $R_{G,\lambda}$ shall be zero at the observing wavelength, λ_{obs}. This leads to a condition on the glass to be used and to an analytical expression for the glass thickness.

Evaluating equation (12), $\frac{\partial R_{G,\lambda}}{\partial\lambda}=0$ results in

$$T=\frac{D}{n_{Fs}}\cdot\left(\frac{\partial n_\lambda}{\partial\lambda}\right)\cdot\left[\frac{\partial N_\lambda}{\partial\lambda}-\frac{\partial n_\lambda}{\partial\lambda}\cdot\frac{N_{\lambda_{Fs}}}{n_{\lambda_{Fs}}}\right]^{-1} \tag{13}$$

and $\frac{\partial^2 R_{G,\lambda}}{\partial^2\lambda}=0$ leads to

$$T=\frac{D}{n_{Fs}}\cdot\left(\frac{\partial^2 n_\lambda}{\partial^2\lambda}\right)\cdot\left[\frac{\partial^2 N_\lambda}{\partial^2\lambda}-\frac{\partial^2 n_\lambda}{\partial^2\lambda}\cdot\frac{N_{\lambda_{Fs}}}{n_{\lambda_{Fs}}}\right]^{-1} \tag{14}$$

Equations (13) and (14) must result in the same thickness T which results in a condition on the glass index of refraction:

$$C_G = \left(\frac{\partial N_\lambda}{\partial \lambda} \Big/ \frac{\partial^2 N_\lambda}{\partial^2 \lambda} \right)_{\lambda_{obs}} \quad \text{shall be equal to} \quad C_A = \left(\frac{\partial n_\lambda}{\partial \lambda} \Big/ \frac{\partial^2 n_\lambda}{\partial^2 \lambda} \right)_{\lambda_{obs}} \tag{15}$$

C_A can be calculated using the formula given by J.C.Owens [8]. C_G is obtained by fitting the measured values of the glass refractive index given in catalogues [7,9] by a polynomial from which the first and second derivatives are computed.

A plot of C_G and C_A is presented figure 4 and shows how the best glass can be chosen out of a given set in order to fulfil condition (15). For a given observing wavelength, the best glass is the one whose C_G is closest to C_A. For example BaF50 seems to be particularly suited at 0.6µm whereas BK7 fulfils better the criteria at 0.4 µm. In order to verify this statement, the residual optical path difference, $R_{G,\lambda}$, is plotted figure 5 after correction with BaF50, for an observing wavelength λ_{obs}=0.6µm and a delay D=120m. As foreseen, its slope is close to zero at 0.6µm. The mean and rms of the residual optical path difference, both calculated over the observing bandwidth $\Delta\lambda$=100nm, are respectively presented in figures 6 and 7.

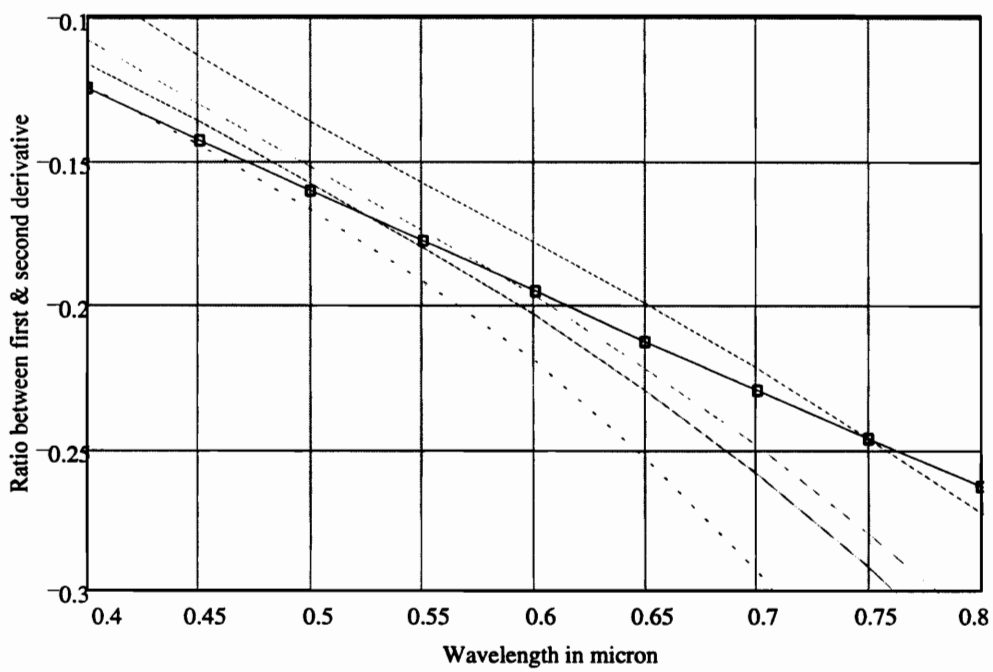

Fig. 4: Representation of minimal slope criteria by a graph. C_A is represented by the solid line with squares whereas C_G is plotted for 4 glasses. Starting from bottom to top at 0.7µm: BK7, BaLF3, BaF50, SF6.

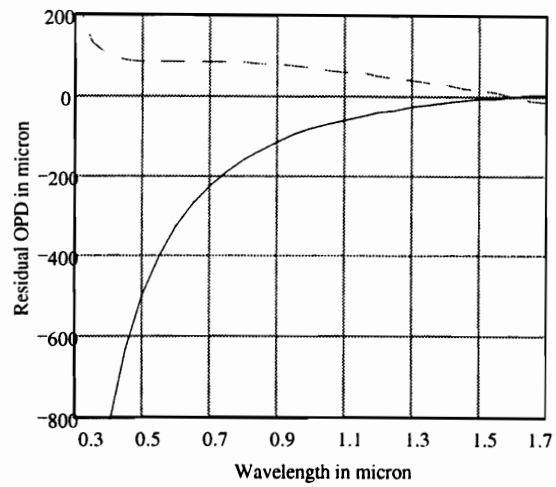

Fig. 5: Residual without glass compensation (solid line) and after with BaF50(dashed line), for a 120m Delay and λ_{obs}=0.6μm.

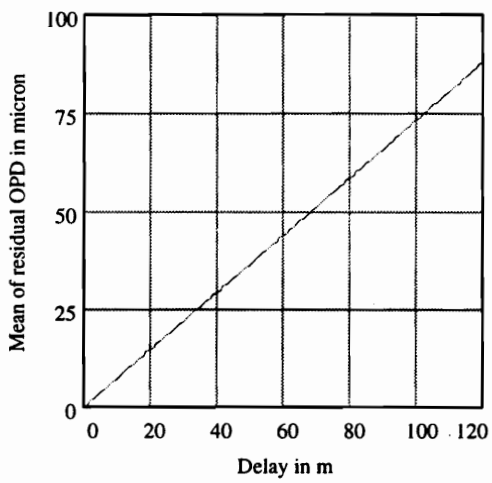

Fig. 6: $\overline{R_{G,\lambda}}$: mean residual OPD of BaF50 calculated over Δλ=100nm, for λ_{obs} =0.6μm;

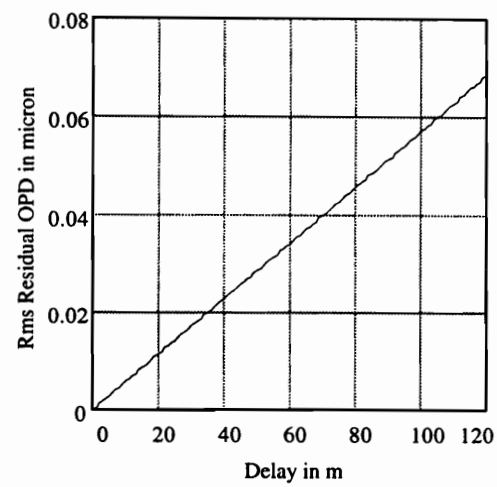

Fig. 7: Corresponding Rms of residual OPD calculated over Δλ=100nm for BaF50.

3.2. Contrast Improvement by offset compensation

At this point, we have selected glass whose thickness has been tuned to obtain a flat residual curve around λ_{obs} (Figure 5). This does not yet assure a maximum contrast as seen by the instrument in the observing bandwidth because no condition on the group delay at λ_{obs} , noted $OPD_g(\lambda_{obs})$, has been imposed.

In order to recover a maximum contrast, $OPD_g(\lambda_{obs})$ must be zeroed. This can be performed by creating an internal path inside the fringe sensor. Thus, when the fringe tracking loop is closed, delay lines are positioned where $OPD_g(\lambda_{obs})=0$ as seen by the instrument. This offset is typically some hundred microns and we do not consider second order dispersion effects due to such a small supplementary air path.

Let us assume that the fringe sensor operates in a sufficiently narrow bandwidth to neglect dispersion across its bandwidth. Thus, the fringe sensor tracks the position $OPD_g(\lambda_{Fs})=OPD(\lambda_{Fs})=0$. In order to

compute the maximum contrast after glass and offset correction, i.e. for $OPD_g(\lambda_{obs})=0$, we use equation (11) where we add to the residual phase optical path difference, $R_{G,\lambda}$, the offset :

$$\zeta = n_{\lambda_{obs}} .[\, X_{Fs} - X_{g,obs}\,] = \left[\frac{D+(N_{\lambda_{Fs}} - n_{\lambda_{Fs}}).T}{n_{\lambda_{Fs}}} - \frac{D+(N_{g,\lambda_{obs}} - n_{g,\lambda_{obs}}).T}{n_{g,\lambda_{obs}}} \right] \cdot n_{\lambda_{obs}} . D$$

The terms X_{Fs} and $X_{g,obs}$ are the geometric positions of the delay lines which respectively give $OPD(\lambda_{Fs})=0$ and $OPD_g(\lambda_{obs})=0$. The subscript "g" refers to the group refractive index [10]. ζ corresponds to the offset needed on the fringe sensor to recover the maximum fringe contrast as seen by the instrument at λ_{obs}.

In practice, dispersion will also occur across the fringe sensor's bandwidth. Firstly, it will lower the fringe contrast as seen by the sensor, i.e. to degrade its performance in terms of magnitude limit. This effect is not considered here. Secondly, the reference OPD around which the fringe sensor tracks will be shifted from $OPD(\lambda_{Fs})=0$ to $OPD_g(\lambda_{Fs})=0$. For the sake of clarity, we do not consider this shift in this paper. This does not influence our conclusion since a supplementary offset inside the fringe sensor can always be introduced so that $OPD(\lambda_{Fs})=0$.

The corrected fringe contrast for λ_{obs}=0.6µm with BaF50 appears in figure 8 and is compared to the contrast obtained using BK7. The latter is clearly reduced which confirms the applicability of the glass selection criteria.

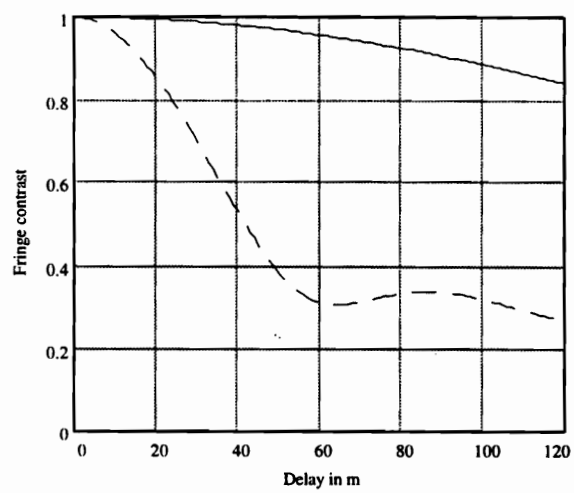

Fig. 8: Fringe contrast after glass correction (BaF50 solid line, BK7 dashed line) for λ_{obs}=0.6µm and $\Delta\lambda$=100nm.

A more general picture of the criteria's efficiency is presented in figures 9 and 10 where the fringe contrast, obtained with the initial set of glasses is included. Three bandwidth, 10, 50 and 100nm were considered at two different observing wavelength, 0.4 µm and 0.6µm. These graphs show that all glasses have a good impact on the fringe contrast for an observing window less than 10nm. However, as soon as the bandwidth is increased, the selection criteria demonstrates its efficiency by pointing out the glass which provides the best fringe contrast. The somehow better general results at 0.6 µm are due to the shorter distance to λ_{Fs} which tends to reduce the residual OPD. Depending on λ_{obs}, the results of the optimal dispersion corrections are summarised for the visible in table 1.

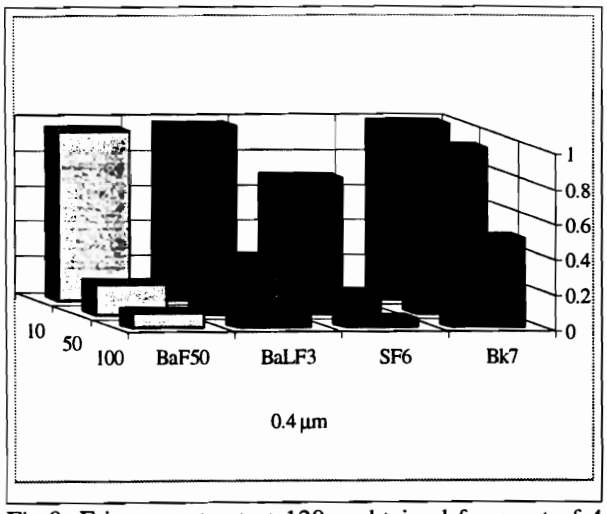

Fig.9 :Fringe contrast at 120m obtained for a set of 4 glasses as a function of 3 observing window (10,50 and 100nm). λ_{obs} =0.4 µm.

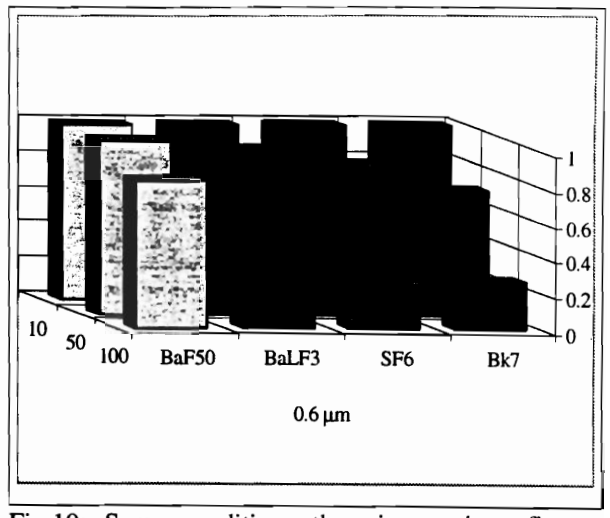

Fig.10: Same conditions than in previous figure except that λ_{obs} = 0.6µm.

λ_{obs} in µm	Best compensation	Contrast at D=120m for Δλ : 50 nm	100nm	Thickness in mm/m of D	Offset in µm needed at D= 120m to cancel $OPD_g(\lambda obs)$
0.40	BK7	0.94	0.5	0.3	255
0.50	BaLF3	0.99	0.71	0.2	117
0.60	BaF50	0.99	0.84	0.15	88
0.75	SF6	0.99	0.99	0.076	34

Table 1

The same method has been applied to find an appropriate glass capable of dispersion compensation in the infrared K band (2.0-2.4 µm). A full correction over the K band is possible using ZnSe which is not hygroscopic. With C_A(2.2µm)=-0.705, we have:

Type of Glass	Selection criteria: $\left(\frac{C_G}{C_A}\right)_{2.2\mu m}$ in %	Contrast at D= 120m, λ_{obs} =2.2µm; Δλ=400nm	Thickness in mm/m of D	Offset needed at D= 120m to cancel $OPD_g(\lambda obs)$	Transmission in % /Water solubility
No Glass correction	N/A	0.8	N/A	30 µm	N/A
ZnSe	95%	>0.99	0.02	180 nm	65% / none
KBr	52%	0.98	0.11	3 µm	90% / 53.5gm for 100gm water at 0°C

Table 2

4. Conclusion

A new glass selection criteria has been presented for longitudinal dispersion compensation applied to the Very Large Telescope Interferometer, with the aim to compensate over a relatively large observing bandwidth. This method has been applied both in the visible and in the infrared (K-band) where the correcting glass was optimised for the observing wavelength and the spectral bandwidth. Results were translated in terms of fringe contrast for which a fairly straightforward formula, applicable in the large bandwidth case, has been developed. This study indicates that a single glass can be used for VLTI with a differential air path of 120m.

5. References

1. J.M. Beckers,"Planning the VLT interferometer",The Messenger, No 60, ESO, 1990
2. J.Gay et al., "L.A.M.P: a concept for the E.S.O VLTI fringe sensor", SPIE Vol.2200 Amplitude and Intensity Spatial Interferometry, Hawaii, 1994.
3. L.Koechlin,"The I2T Interferometer", NOAO/ESO Conference on High resolution imaging by interferometry, Garching, Germany, 15-18 March 1988.
4. B.Koehler et al." Engineering aspects of the environmental factors affecting the VLTI performance", SPIE Vol.2200 Amplitude and Intensity Spatial Interferometry, Hawaii, 1994.
5. M.Lacasse,"Glass compensation for an air filled delay line", NOAO/ESO Conference on High resolution imaging by interferometry, Garching, Germany, 15-18 March 1988.
6. S.Lévêque et al." Measurement of optical path fluctuations due to internal seeing for the VLTI", SPIE Vol.2566 Advanced Imaging Technologies and Commercial Applications, San Diego, 1995.
7. Merck Ltd glass catalogue, Poole BH12 4NN, England "Crystran,Optical crystals"
8. J.C Owens, "Optical refractive index of air: dependence on pressure, temperature and composition", Applied Optics, vol 6, No 1, January 1967, p.51
9. Schott-Glass catalogue , 6500 Mainz,Germany,"Optical Glass catalogue"
10. W.H Steel, "Interferometry", Cambridge university press, second edition, 1983.
11. W.J.Tango,"Dispersion in stellar interferometry",Applied Optics, vol.29, No.4, 1990,p.516
12.T.A.Ten Brummelaar, " Differential path considerations in optical stellar interferometry", Applied optics, vol.34, No.13, 1995,p.2215
13. O. von der Lühe et al."The interferometric mode of the ESO VLT", SPIE Vol.2200 Amplitude and Intensity Spatial Interferometry, Hawaii, 1994.

NAME | M.S.